# A tunable waveguide-coupled cavity design for scalable interfaces to solid-state quantum emitters

Sara L. Mouradian, and Dirk Englund

Citation: APL Photonics **2**, 046103 (2017);
View online: https://doi.org/10.1063/1.4978204
View Table of Contents: http://aip.scitation.org/toc/app/2/4
Published by the American Institute of Physics

APL PHOTONICS **2**, 046103 (2017)

# A tunable waveguide-coupled cavity design for scalable interfaces to solid-state quantum emitters

Sara L. Mouradian[a] and Dirk Englund[b]
*Department of Electrical Engineering and Computer Science, Massachusetts Institute of Technology, Cambridge, Massachusetts 02139, USA*

(Received 26 October 2016; accepted 23 February 2017; published online 14 March 2017)

Photonic nanocavities in diamond have emerged as useful structures for interfacing photons and embedded atomic color centers, such as the nitrogen vacancy center. Here, we present a hybrid nanocavity design that enables (i) a loaded quality factor exceeding 50 000 (unloaded $Q > 10^6$) with 75% of the enhanced emission collected into an underlying waveguide circuit, (ii) MEMS-based cavity spectral tuning without straining the diamond, and (iii) the use of a diamond waveguide with straight sidewalls to minimize surface defects and charge traps. This system addresses the need for scalable on-chip photonic interfaces to solid-state quantum emitters.  [http://dx.doi.org/10.1063/1.4978204]

Solid state quantum emitters, such as defects in diamond or quantum dots in III-V materials, have been demonstrated as high quality single photon sources and quantum memories. The entanglement rate between quantum repeaters in a quantum communication network, or between quantum bits (qubits) in a distributed quantum computation platform, scales with the square of the collection rate of indistinguishable photons from each node. Thus, the cavity enhancement of the transition of interest can significantly increase secure communication rates or the maximum size of an entangled network. Photonic crystal (PhC) cavities are an attractive choice for enhancing solid state qubits as they provide high quality factors ($Q$) and wavelength-scale mode volumes ($V$) with direct patterning of the host material. Cavity enhancement of quantum dots in III-V materials has enabled strong light-matter coupling[1] and record rates of indistinguishable photons.[2–5] Recent advances in diamond nanofabrication[6] have enabled the fabrication of free-standing photonic crystal cavities in diamond for the enhancement of the zero phonon line (ZPL) transition of silicon vacancy centers[7,8] and negatively charged nitrogen vacancy (NV) centers.[9–19]

However, there are currently two main challenges limiting progress in scaling to multiple coupled emitter-cavity systems for distributed quantum networks. In order to improve the entanglement rate, the cavity design must not only enhance the emission of the desired transition via a high $Q$ mode at the transition frequency but more importantly increase the overall collection rate of that transition. Thus the loss pathways of the cavity must be engineered to funnel the enhanced light into a single useable mode, such as a waveguide mode for further routing and manipulation. Secondly, fabrication inconsistencies across a single chip cause a spread in the resonant frequencies of the final devices that can severely decrease the enhancement of the desired transition. Thus, post-fabrication tuning at each individual node is necessary.

In this letter, we present a hybrid cavity design that addresses both of these challenges: 75% of the mode at each cavity is coupled into a single waveguide mode of the underlying photonic integrated circuit (PIC) that connects all nodes, and the frequency is tunable over 10 linewidths while maintaining a $Q$ factor within 50% of the maximum value.

[a]smouradi@mit.edu
[b]englund@mit.edu

 

While the design presented in this paper can be easily modified to enhance other solid state emitters, or connect with other PIC systems, we present a design to enhance the NV center's ZPL in a diamond node integrated into an Aluminum Nitride (AlN) PIC.

The NV center has exceptional spin properties for a solid state quantum emitter, with electron spin states with second-scale coherence times.[20,21] The electron spin state can also be optically initialized, manipulated, and measured,[22] and can be mapped onto nearby auxiliary nuclear memories[23] for increased coherence times. The long coherence time and ease of state measurement and manipulation enables entanglement generation and state teleportation between two spatially separate quantum memories.[24–26] However, the reported entanglement rates remain well below even the nuclear spin decoherence rate, eliminating the possibility of creating entanglement over three or more nodes. This low entanglement rate is currently limited by the small probability of collecting a photon coherent with the spin state into the frequency and spatial mode needed for entanglement due to low collection efficiency, spectral diffusion, and phonon interactions present even at cryogenic temperatures. Thus, cavity enhanced collection into a single frequency and spatial mode is essential to scale entanglement from two NV centers to three or more. AlN is chosen to create the optical band-gap at the cavity region—and as the backbone PIC material—as it has a wide direct band-gap (~6.1 eV at 4 K) that allows low-loss single-mode operation at the NV ZPL wavelength (637 nm). Moreover, its favorable piezoelectric properties have made it a widely used material for free-standing nanoelectromechanical (NEMS) devices,[27,28] and electro-optic and frequency conversion devices[29,30] have been demonstrated, making it a promising platform for reconfigurable quantum circuits that can interface with fibers for long-distance quantum communication. This active ability also enables the NEMS needed to tune the cavity frequency, as discussed below.

The AlN backbone consists of single mode waveguides with all beam splitters and active components needed for routing the optical signal between cavity nodes. As indicated in the schematic of Figure 1(a) and the cross section in Figure 1(b), the substrate at the cavity region is etched away to leave the AlN suspended in air. A diamond waveguide containing a single, well-characterized NV center is placed into the cavity region. The diamond waveguide is suspended at the cavity region, with both ends resting on the substrate and locked into AlN alignment features.

As shown in Figure 1(a), the cavity region consists of two suspended parallel AlN waveguides with a height $H/\lambda_{NV} = 0.345$ and width $W/\lambda_{NV} = 0.383$, where $\lambda_{NV} = 637$ nm is the free-space ZPL wavelength. These are patterned with periodic holes with constant spacing ($a/\lambda_{NV} = 0.356$) and constant radius ($r/a = 0.295$). A diamond slab with the same height as the AlN layer containing a single NV center at the center of the beam is centered between the two AlN beams ($D_1 = D_2 = 0.235\lambda_{NV}$). The width of the suspended diamond membrane increases parabolically from $W_1/\lambda_{NV} = 0.157$ to $W_2/\lambda_{NV} = 0.314$ over 7 periods. The periodic patterning of the two AlN waveguides creates a bandgap in the $x$ direction. The increased width of the diamond membrane at the center of the structure increases the effective refractive index in a localized spot in the otherwise periodic structure. Moreover, the diamond refractive index ($n_{dmd} = 2.42$) is higher than that of AlN ($n_{AlN} = 2.10$), and so the mode resides in the diamond as seen in the energy distribution ($|E|^2$) shown in Figure 1(c). The gentle

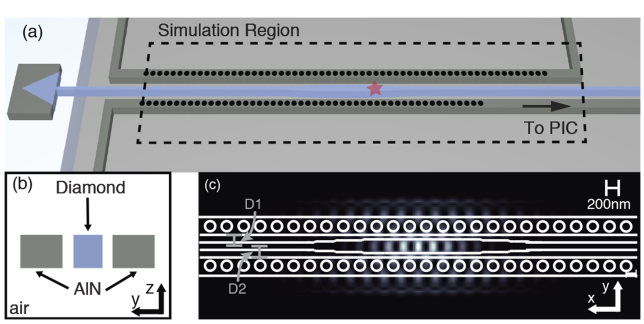


FIG. 1. (a) Structure of the hybrid cavity. Two suspended AlN beams (gray) periodically patterned with holes sit on either side of a width-modulated diamond (blue). (b) Cross section through $x = 0$ plane of the cavity. (c) Unloaded cavity mode profile ($|E|^2$).

parabolic width increase reduces scattering,[31] and finite difference time domain (FDTD) simulations show a radiation-limited $Q$ factor of >1 million with 50 holes on either side of the center of the cavity.

FDTD simulations reveal a mode volume of $V \approx 10(\lambda_{NV}/n_{dmd})^3$. Due to the large transverse extent of the hybrid structure, this mode volume is larger than other nanobeam cavity designs, which provide mode volumes on the order of $(\lambda/n)^3$. However, the high $Q$ ensures a large Purcell enhancement for an optimally placed and oriented NV center. The mode maximum is at the center of the structure, or 110 nm in depth and 100 nm from each side of the diamond. The mode is within 90% of the maximum within ±20 nm, ±30 nm, and ±60 nm for the $x$, $y$, and $z$ directions, respectively.

The central positioning of the NV center (≥100 nm from each surface) is also beneficial for the optical properties of the NV. Although the NV exhibits long-lived electronic spin states, they are especially sensitive to stray electric fields, and the nanofabrication of PhC cavities can introduce defects in the crystal and on the surface due to the ion bombardment that is necessary to etch the host material. These defects trap charges in unstable configurations that lead to pure dephasing and spectral diffusion that in turn leads to a decrease in entanglement rate due to reduced indistinguishability between photons emitted by distinct emitters. The spectral diffusion of solid state emitters increases with proximity to fabricated surfaces,[12,32] and previous work in bulk diamond has demonstrated lifetime limited linewidths of NVs 100 nm from the surface,[33] suggesting that this design could provide the same with adequate surface treatment. In this design, the diamond is only minimally patterned, and instead the periodic change in the dielectric environment needed to produce a band gap is provided by the patterning in the AlN.

To efficiently collect the NV emission into the backbone PIC, the cavity must be coupled to the waveguide. The unloaded design described above has a high $Q$, but the emitted light cannot be efficiently collected into the waveguide as it radiates mainly into the $z$-plane. Thus, despite the large Purcell enhancement due to the high $Q/V$, there is only a marginal increase of light collected into a single AlN waveguide mode over a simpler, broadband architecture of an NV coupled to a single diamond waveguide mode that is adiabatically tapered to transfer the optical mode to the underlying PIC mode.[32] To increase the collection enhancement, the cavity is loaded into a single AlN waveguide mode by reducing the number of holes on one of the four sides of the cavity, as seen in Fig. 2(a). In general, the fraction of emission into the waveguide can be estimated from the ratio $F = Q_l/(Q_l + Q_i)$ where $Q_i$ is the intrinsic Q factor, and $Q_l$ is the loaded $Q$ factor. However, modifying the cavity geometry can also increase scattering into other loss pathways. Moreover, the figure of merit of interest is the overall collection enhancement, which is a function of $Q$ and $F$. Therefore, we performed detailed FDTD simulations to measure the collection enhancement into the waveguide port. As seen in Fig. 2(a), the collection enhancement is maximized when the number of holes leading to the output waveguide is $N_{out} = 16$. At this configuration, the loaded $Q$ is 55 000, with 75% of the light coupled into the waveguide as calculated with FDTD simulations. The collection spectra into

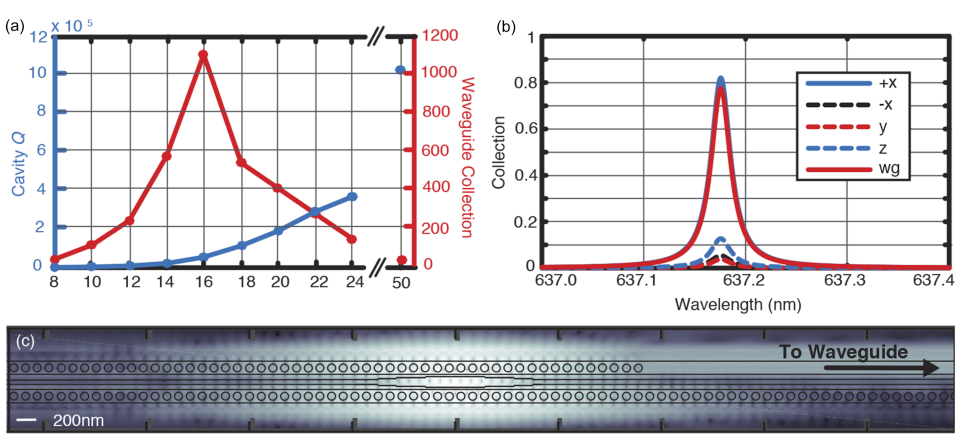


FIG. 2. (a) The enhancement of collection into the waveguide mode vs the number of holes leading to the loading waveguide. (b) The spectrally resolved intensity fraction collected into the waveguide mode as well as the losses into the $-x$, $y$, and $z$ planes at $N_{\text{out}} = 16$. (c) Loaded cavity mode profile $\log(|E|^2)$.

the waveguide, as well as into the $y$ and $z$ planes are shown in Fig. 2(b). Fig. 2(c) shows the mode profile ($\log(|E|^2)$) of the loaded cavity, with clear coupling into the bottom right waveguide.

For high fidelity entanglement between two NV centers, they both must emit into the same lifetime-limited frequency mode. The ZPL transition frequency of 2 or more NV centers can be tuned to overlap via the Stark effect.[34] However, the cavities' resonances must also be at the same frequencies. Unfortunately, fabrication imperfections across a single chip can cause inhomogeneities in the resonant frequencies. Therefore, it is necessary to tune the frequency of the cavity post-fabrication without a significant drop in the quality factor of the cavity. Previous works have demonstrated cavity tuning in other material systems. For instance, the fast and reversible tuning of PhC cavities in semiconductors such as Si and GaAs has been demonstrated via injection of free carriers, either electrically[35] or via two photon absorption.[36] However, PN junctions are notoriously difficult to make in diamond and doping the diamond may have deleterious effects on the NV center. Previous cavity results in diamond[8,14] have used gas adsorption and sublimation to tune a cavity's resonant frequency, but this approach affects all cavities on the chip simultaneously and cannot be easily used to stabilize the resonant frequencies of many cavities on the same chip over a long period of time.

Works in other material systems employed nano-electrical-mechanical systems (NEMS) to couple two cavity modes[37,38] or modify the evanescent field of the cavity mode to induce wavelength shifts.[39–41] This is not currently feasible in an all-diamond system as large-scale free-standing membranes are not widely available, and moving the diamond would cause strain which would shift the NV center's optical transitions.[42] In the hybrid design presented in this paper, the AlN layer can provide the needed NEMS functionality using electrostatic or piezoelectric[27,28] actuation. FDTD simulations show that displacing the two patterned AlN beams changes the cavity's effective refractive index, and thus the resonant frequency. The tuning simulations were performed on the loaded cavity. Moving the waveguide-coupled AlN beam a certain distance ($D_1$) provides different tuning than moving the non-coupled beam the same distance ($D_2 = D_1$). Figure 3(a) summarizes the results showing the effect of beam displacements on resonant frequency and $Q$, plotted against ($D_2 - D_1$). Figure 3(b) demonstrates that the cavity can be tuned over 10 linewidths while maintaining $Q \geq 0.5\ Q_{\max}$. While this device's tuning range is small due to the high $Q$, it allows the individual tuning of multiple cavities on the same chip with no crosstalk. If necessary, coarse tuning of cavities can be accomplished by a variety of other techniques such as photochromic[43] or chalcogenide index-changing[44] materials. The cavity fine-tuning, as proposed here using NEMS actuation, is required to tune and maintain many high-Q on-chip cavities on resonance for the realization of on-chip quantum networks and entanglement distribution in envisioned quantum repeater architectures.[45]

Finally, this hybrid cavity design is compatible with the scalable hybrid assembly of a photonic backbone populated with pre-selected quantum nodes.[32,46–48] The proposed approach requires careful alignment between the diamond and AlN components. Vertical alignment ($z$) is assured by the diamond membrane's physical contact with the plane of the substrate. $x$ alignment must be within ±30 nm to maintain an enhancement ≥90% of the maximum. Various pick-and-placement techniques have already been demonstrated with excellent in-plane alignment, including optical microscopy with better than 200 nm in-plane tolerance[32,49] and scanning-electron microscope based alignment with 25 nm tolerance,[50–53] aided by lithographically defined alignment structures as indicated in

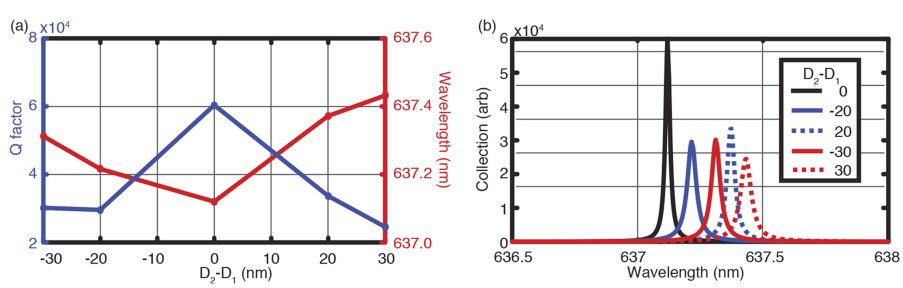


FIG. 3. (a) Resonant wavelength and $Q$ factor as the two AlN DBRs are displaced. (b) Cavity spectrum for different positions of the AlN beams.

Figure 1(a). Finally, any remaining error is correctable *in situ* using AlN NEMS actuators in $x$ and $y$ directions.

In conclusion, we introduced a novel hybrid cavity design that enhances the collection of photons from a transition of an embedded quantum emitter that is at the resonant frequency of the cavity. This is achieved by loading a high-$Q$ cavity directly into a single mode PIC network. Moreover, the emitter remains ≥100 nm away from every surface, reducing spectral diffusion due to trapped charges on the surface. Finally, NEMS actuation permits the reversible and stable tuning of the resonant frequency. The implementation of this design across a multi-node PIC will enable efficient multi-qubit entanglement across the PIC.

This research was supported in part by the Army Research Laboratory Center for Distributed Quantum Information (CDQI). S.M. was supported in part by IQUISE, in part by the NSF EFRI-ACQUIRE program Scalable Quantum Communications with Error-Corrected Semiconductor Qubits, and in part by the AFOSR Quantum Memories MURI. D.E. acknowledges partial support from the STC Center for Integrated Quantum Materials (CIQM), NSF Grant No. DMR-1231319. We thank Mikkel Heuck and Tim Schröder for valuable discussions.

[1] D. Englund, A. Faraon, I. Fushman, N. Stoltz, P. Petroff, and J. Vučković, "Controlling cavity reflectivity with a single quantum dot," Nature **450**, 857–861 (2007).
[2] C. Santori, D. Fattal, J. Vučković, G. S. Solomon, and Y. Yamamoto, "Indistinguishable photons from a single-photon device," Nature **419**, 594–597 (2002).
[3] N. Somaschi, V. Giesz, L. De Santis, J. C. Loredo, M. P. Almeida, G. Hornecker, S. L. Portalupi, T. Grange, C. Anton, J. Demory *et al.*, "Near-optimal single-photon sources in the solid state," Nat. Photonics **10**, 340 (2016).
[4] H. Wang, Z.-C. Duan, Y.-H. Li, S. Chen, J.-P. Li, Y.-M. He, M.-C. Chen, Y. He, X. Ding, C.-Z. Peng *et al.*, "Near-transform-limited single photons from an efficient solid-state quantum emitter," Phys. Rev. Lett. **116**, 213601 (2016).
[5] X. Ding, Y. He, Z.-C. Duan, N. Gregersen, M.-C. Chen, S. Unsleber, S. Maier, C. Schneider, M. Kamp, S. Höfling *et al.*, "On-demand single photons with high extraction efficiency and near-unity indistinguishability from a resonantly driven quantum dot in a micropillar," Phys. Rev. Lett. **116**, 020401 (2016).
[6] T. Schröder, S. L. Mouradian, J. Zheng, M. E. Trusheim, M. Walsh, E. H. Chen, L. Li, I. Bayn, and D. Englund, "Quantum nanophotonics in diamond [invited]," J. Opt. Soc. Am. B **33**, B65–B83 (2016).
[7] J. Riedrich-Möller, C. Arend, C. Pauly, F. Mücklich, M. Fischer, S. Gsell, M. Schreck, and C. Becher, "Deterministic coupling of a single silicon-vacancy color center to a photonic crystal cavity in diamond," Nano Lett. **14**, 5281–5287 (2014).
[8] A. Sipahigil, R. E. Evans, D. D. Sukachev, M. J. Burek, J. Borregaard, M. K. Bhaskar, C. T. Nguyen, J. L. Pacheco, H. A. Atikian, C. Meuwly *et al.*, "An integrated diamond nanophotonics platform for quantum optical networks," Science **354**, 847 (2016).
[9] J. Wolters, A. W. Schell, G. Kewes, N. Nüsse, M. Schoengen, H. Döscher, T. Hannappel, B. Löchel, M. Barth, and O. Benson, "Enhancement of the zero phonon line emission from a single nitrogen vacancy center in a nanodiamond via coupling to a photonic crystal cavity," Appl. Phys. Lett. **97**, 141108 (2010).
[10] D. Englund, B. Shields, K. Rivoire, F. Hatami, J. Vuckovic, H. Park, and M. D. Lukin, "Deterministic coupling of a single nitrogen vacancy center to a photonic crystal cavity," Nano Lett. **10**, 3922–3926 (2010).
[11] A. Faraon, P. E. Barclay, C. Santori, K.-M. C. Fu, and R. G. Beausoleil, "Resonant enhancement of the zero-phonon emission from a colour centre in a diamond cavity," Nat. Photonics **5**, 301–305 (2011).
[12] A. Faraon, C. Santori, Z. Huang, V. M. Acosta, and R. G. Beausoleil, "Coupling of nitrogen-vacancy centers to photonic crystal cavities in monocrystalline diamond," Phys. Rev. Lett. **109**, 033604 (2012).
[13] J. Riedrich-Möller, L. Kipfstuhl, C. Hepp, E. Neu, C. Pauly, F. Mücklich, A. Baur, M. Wandt, S. Wolff, M. Fischer, S. Gsell, M. Schreck, and C. Becher, "One- and two-dimensional photonic crystal microcavities in single crystal diamond," Nat. Nanotechnol. **7**, 69–74 (2012).
[14] L. Li, T. Schröder, E. H. Chen, M. Walsh, I. Bayn, J. Goldstein, O. Gaathon, M. E. Trusheim, M. Lu, J. Mower *et al.*, "Coherent spin control of a nanocavity-enhanced qubit in diamond," Nat. Commun. **6**, 6173 (2015).
[15] I. Bayn, S. Mouradian, L. Li, J. A. Goldstein, T. Schröder, J. Zheng, E. H. Chen, O. Gaathon, M. Lu, A. Stein, C. A. Ruggiero, J. Salzman, R. Kalish, and D. Englund, "Fabrication of triangular nanobeam waveguide networks in bulk diamond using single-crystal silicon hard masks," Appl. Phys. Lett. **105**, 211101 (2014).
[16] M. J. Burek, Y. Chu, M. S. Z. Liddy, P. Patel, J. Rochman, S. Meesala, W. Hong, Q. Quan, M. D. Lukin, and M. Lončar, "High quality-factor optical nanocavities in bulk single-crystal diamond," Nat. Commun. **5** 5718 (2014).
[17] M. Schukraft, J. Zheng, T. Schröder, S. L. Mouradian, M. Walsh, M. E. Trusheim, H. Bakhru, and D. R. Englund, "Invited article: Precision nanoimplantation of nitrogen vacancy centers into diamond photonic crystal cavities and waveguides," APL Photonics **1**, 020801 (2016).
[18] J. C. Lee, D. O. Bracher, S. Cui, K. Ohno, C. A. McLellan, X. Zhang, P. Andrich, B. Alemán, K. J. Russell, A. P. Magyar *et al.*, "Deterministic coupling of delta-doped nitrogen vacancy centers to a nanobeam photonic crystal cavity," Appl. Phys. Lett. **105**, 261101 (2014).
[19] B. J. M. Hausmann, B. J. Shields, Q. Quan, Y. Chu, N. P. De Leon, R. Evans, M. J. Burek, A. S. Zibrov, M. Markham, D. J. Twitchen *et al.*, "Coupling of nv centers to photonic crystal nanobeams in diamond," Nano Lett. **13**, 5791–5796 (2013).

[20] P. C. Maurer, G. Kucsko, C. Latta, L. Jiang, N. Y. Yao, S. D. Bennett, F. Pastawski, D. Hunger, N. Chisholm, M. Markham, D. J. Twitchen, J. I. Cirac, and M. D. Lukin, "Room-temperature quantum bit memory exceeding one second," Science **336**, 1283–1286 (2012).
[21] N. Bar-Gill, L. M. Pham, A. Jarmola, D. Budker, and R. L. Walsworth, "Solid-state electronic spin coherence time approaching one second," Nat. Commun. **4**, 1743 (2013).
[22] P. Neumann, J. Beck, M. Steiner, F. Rempp, H. Fedder, P. R. Hemmer, J. Wrachtrup, and F. Jelezko, "Single-shot readout of a single nuclear spin," Science **329**, 542–544 (2010).
[23] M. V. Gurudev Dutt, L. Childress, L. Jiang, E. Togan, J. Maze, F. Jelezko, A. S. Zibrov, P. R. Hemmer, and M. D. Lukin, "Quantum register based on individual electronic and nuclear spin qubits in diamond," Science **316**, 1312–1316 (2007).
[24] W. Pfaff, B. Hensen, H. Bernien, S. B. van Damm, M. S. Blok, T. H. Taminiau, M. J. Tiggelman, R. N. Schouten, M. Markham, D. J. Twitchen, and R. Hanson, "Unconditional quantum teleportation between distant solid-state quantum bits," Science **345**, 532–535 (2014).
[25] H. Bernien, B. Hensen, W. Pfaff, G. Koolstra, M. S. Blok, L. Robledo, T. H. Taminiau, M. Markham, D. J. Twitchen, L. Childress, and R. Hanson, "Heralded entanglement between solid-state qubits separated by three metres," Nature **497**, 86–90 (2013).
[26] B. Hensen, H. Bernien, A. E. Dréau, A. Reiserer, N. Kalb, M. S. Blok, J. Ruitenberg, R. F. L. Vermeulen, R. N. Schouten, C. Abellán *et al.*, "Loophole-free bell inequality violation using electron spins separated by 1.3 kilometres," Nature **526**, 682–686 (2015).
[27] R. B. Karabalin, M. H. Matheny, X. L. Feng, E. Defaÿ, G. Le Rhun, C. Marcoux, S. Hentz, P. Andreucci, and M. L. Roukes, "Piezoelectric nanoelectromechanical resonators based on aluminum nitride thin films," Appl. Phys. Lett. **95**, 103111 (2009).
[28] N. Sinha, G. E. Wabiszewski, R. Mahameed, V. V. Felmetsger, S. M. Tanner, R. W. Carpick *et al.*, "Piezoelectric aluminum nitride nanoelectromechanical actuators," Appl. Phys. Lett. **95**, 053106 (2009).
[29] X. Guo, C.-L. Zou, H. Jung, and H. X. Tang, "On-chip strong coupling and efficient frequency conversion between telecom and visible optical modes," Phys. Rev. Lett. **117**, 123902 (2016).
[30] C.-L. Zou, X. Han, L. Jiang, and H. X. Tang, "Cavity piezomechanical strong coupling and frequency conversion on an aluminum nitride chip," Phys. Rev. A **94**, 013812 (2016).
[31] Y. Akahane, T. Asano, B.-S. Song, and S. Noda, "High-q photonic nanocavity in a two-dimensional photonic crystal," Nature **425**, 944–947 (2003).
[32] S. L. Mouradian, T. Schröder, C. B. Poitras, L. Li, J. Goldstein, E. H. Chen, M. Walsh, J. Cardenas, M. L. Markham, D. J. Twitchen, M. Lipson, and D. Englund, "Scalable integration of long-lived quantum memories into a photonic circuit," Phys. Rev. X **5**, 031009 (2015).
[33] Y. Chu, N. P. De Leon, B. J. Shields, B. Hausmann, R. Evans, E. Togan, M. J. Burek, M. Markham, A. Stacey, A. S. Zibrov *et al.*, "Coherent optical transitions in implanted nitrogen vacancy centers," Nano Lett. **14**, 1982–1986 (2014).
[34] Ph. Tamarat, T. Gaebel, J. R. Rabeau, M. Khan, A. D. Greentree, H. Wilson, L. C. L. Hollenberg, S. Prawer, P. Hemmer, F. Jelezko *et al.*, "Stark shift control of single optical centers in diamond," Phys. Rev. Lett. **97**, 083002 (2006).
[35] I. Fushman, D. Englund, J. Vuckovic, E. Waks, N. Stoltz, and P. Petroff, "Ultra fast nonlinear optical tuning of photonic crystal cavities," in *Conference on Lasers and Electro-Optics* (Optical Society of America, 2007), p. CFQ2.
[36] T. Tanabe, M. Notomi, S. Mitsugi, A. Shinya, and E. Kuramochi, "All-optical switches on a silicon chip realized using photonic crystal nanocavities," Appl. Phys. Lett. **87**, 151112 (2005).
[37] X. Chew, G. Zhou, H. Yu, F. Siong Chau, J. Deng, Y. Chong Loke, and X. Tang, "An in-plane nano-mechanics approach to achieve reversible resonance control of photonic crystal nanocavities," Opt. Express **18**, 22232–22244 (2010).
[38] I. W. Frank, P. B. Deotare, M. W. McCutcheon, and M. Lončar, "Programmable photonic crystal nanobeam cavities," Opt. Express **18**, 8705–8712 (2010).
[39] X. Chew, G. Zhou, F. Siong Chau, and J. Deng, "Enhanced resonance tuning of photonic crystal nanocavities by integration of optimized near-field multitip nanoprobes," J. Nanophotonics **5**, 059503 (2011).
[40] F. Tian, G. Zhou, F. Siong Chau, J. Deng, Y. Du, X. Tang, R. Akkipeddi, and Y. C. Loke, "Tuning of split-ladder cavity by its intrinsic nano-deformation," Opt. Express **20**, 27697–27707 (2012).
[41] X. Chew, G. Zhou, F. Siong Chau, J. Deng, X. Tang, and Y. C. Loke, "Dynamic tuning of an optical resonator through mems-driven coupled photonic crystal nanocavities," Opt. Lett. **35**, 2517–2519 (2010).
[42] A. Batalov, V. Jacques, F. Kaiser, P. Siyushev, P. Neumann, L. J. Rogers, R. L. McMurtrie, N. B. Manson, F. Jelezko, and J. Wrachtrup, "Low temperature studies of the excited-state structure of negatively charged nitrogen-vacancy color centers in diamond," Phys. Rev. Lett. **102**, 195506 (2009).
[43] D. Sridharan, E. Waks, G. Solomon, and J. T. Fourkas, "Reversible tuning of photonic crystal cavities using photochromic thin films," Appl. Phys. Lett. **96**, 153303 (2010).
[44] A. Faraon, D. Englund, D. Bulla, B. Luther-Davies, B. J. Eggleton, N. Stoltz, P. Petroff, and J. Vučković, "Local tuning of photonic crystal cavities using chalcogenide glasses," Appl. Phys. Lett. **92**, 043123 (2008).
[45] S. E. Vinay and P. Kok, "Practical repeaters for ultra-long distance quantum communication," preprint arXiv:1607.08140 (2016).
[46] O. Benson, "Assembly of hybrid photonic architectures from nanophotonic constituents," Nature **480**, 193–199 (2011).
[47] I. E. Zadeh, A. W. Elshaari, K. D. Jns, A. Fognini, D. Dalacu, P. J. Poole, M. E. Reimer, and V. Zwiller, "Deterministic integration of single photon sources in silicon based photonic circuits," Nano Lett. **16**, 2289–2294 (2016).
[48] M. D. Birowosuto, A. Yokoo, G. Q. Zhang, K. Tateno, E. Kuramochi, H. Taniyama, M. Takiguchi, M. Notomi *et al.*, "Movable high-q nanoresonators realized by semiconductor nanowires on a si photonic crystal platform," Nat. Mater. **13**, 279–285 (2014).

[49] F. Najafi, J. Mower, N. C. Harris, F. Bellei, A. Dane, C. Lee, X. Hu, P. Kharel, F. Marsili, S. Assefa, K. K. Berggren, and D. Englund, "On-chip detection of non-classical light by scalable integration of single-photon detectors," Nat. Commun. **6**, 5873 (2015).
[50] K. Aoki, H. T. Miyazaki, H. Hirayama, K. Inoshita, T. Baba, K. Sakoda, N. Shinya, and Y. Aoyagi, "Microassembly of semiconductor three-dimensional photonic crystals," Nat. Mater. **2**, 117–121 (2003).
[51] K. Aoki, D. Guimard, M. Nishioka, M. Nomura, S. Iwamoto, and Y. Arakawa, "Coupling of quantum-dot light emission with a three-dimensional photonic-crystal nanocavity," Nat. Photonics **2**, 688–692 (2008).
[52] K. Ishizaki, K. Suzuki, and S. Noda, "Fabrication of 3d photonic crystals toward arbitrary manipulation of photons in three dimensions," in *Photonics* (Multidisciplinary Digital Publishing Institute, 2016), p. 36, Vol. 3.
[53] S. Kawashima, M. Imada, K. Ishizaki, and S. Noda, "High-precision alignment and bonding system for the fabrication of 3-d nanostructures," J. Microelectromech. Syst. **16**, 1140–1144 (2007).